

Submitted to *Energies*. Pages 1 - 21.

OPEN ACCESS

Article

## Three-phase primary control for unbalance sharing between distributed generation units in a microgrid

Tine L. Vandoorn <sup>1,\*</sup>, Jeroen D. M. De Kooning <sup>1</sup>, Jan Van de Vyver <sup>1</sup>, and Lieven Vandevelde <sup>1</sup>,

<sup>1</sup> Dept. of Electrical Energy, Systems & Automation, Ghent University, Sint-Pietersnieuwstraat 41, 9000 Gent, Belgium

\* Author to whom correspondence should be addressed; Tine.Vandoorn@UGent.be, +32 9 264 3422.

Version December 12, 2013 submitted to *Energies*. Typeset by *LaTeX* using class file *mdpi.cls*

**Abstract:** For islanded microgrids, droop-based control concepts have been developed both in single and three-phase variants. The three-phase controllers often assume a balanced network, hence, unbalance sharing and/or mitigation remains a challenging issue. Therefore, in this paper, unbalance is considered in a three-phase islanded microgrid where the distributed generation (DG) units are operated by the voltage-based droop (VBD) control. For this purpose, the VBD control, which has been developed for single-phase systems, is extended for three phase application and an additional control loop is added for unbalance mitigation and sharing. The method is based on an unbalance mitigation scheme by DG units in grid-connected systems, which is altered for usage in grid-forming DG units with droop control. The reaction of the DG units to unbalance is determined by the main parameter of the additional control loop, viz, the distortion damping resistance  $R_d$ . The effect of  $R_d$  on the unbalance mitigation is studied in this paper, i.e., dependent on  $R_d$ , the DG units can be resistive for unbalance (RU) or they can contribute in the weakest phase (CW). The paper shows that the RU method decreases the line losses in the system and achieves better power equalization between the DG unit's phases. However, it leads to a larger voltage unbalance near the loads. The CW method leads to a more uneven power between the DG unit's phases and larger line losses, but a better voltage quality near the load. However, it can negatively affect the stability of the system. In microgrids with multiple DG units, the distortion damping resistance is set such that the unbalanced load can be shared between multiple DG units in an actively controlled manner rather than being determined by the microgrid configuration solely. The unit with the lowest distortion resistance provides relatively more of the unbalanced currents.

**Keywords:** distributed generation, droop controllers, microgrid, unbalance sharing

---

## 24 1. Introduction

25 Microgrids can become incubators of smart grid technologies. These new technologies can be  
26 integrated faster and at a lower cost in microgrids than in the overall electric power system [1], and  
27 they can be specifically selected to meet the specific needs of the local microgrid users. The smart grid  
28 is expected to emerge as a plug-and-play integration of smart grid-connected microgrids [2]. Isolated  
29 microgrids can effectively electrify off-grid areas or “keep the lights on” in times of crisis. Their  
30 small scale, often low load factor (ratio of average and peak power), large share of variable power  
31 sources and the lack of a significant amount of inertia can make isolated microgrid control rather  
32 challenging. However, as isolated microgrids can be regarded as small pilot versions of the future electric  
33 power system, microgrid control is an actual topic [3]. In [3], an overview of microgrid controllers is  
34 provided. A promising control strategy is the droop control, which mimics the conventional control  
35 of the synchronous generators in the transmission system [4,5]. A specific variant of droop control  
36 is the active power/grid voltage ( $P/V$ ) droop controller, based on the predominantly resistive lines in  
37 low-voltage microgrids. Based on the  $P/V$  droop control and further taking into account the large share  
38 of renewable energy sources, the voltage-based droop (VBD) control concept has been presented in [6].  
39 In VBD control, constant-power bands are used to allow for an active participation of the renewables  
40 in the primary microgrid control during critical instants such as a very low load burden. In previous  
41 papers, single-phase microgrids have been considered. In this paper, the VBD controller is extended  
42 for three-phase application keeping its intrinsic advantages, such as maximizing the renewable energy  
43 capture and taking into account the specific nature of the low-voltage isolated microgrids, e.g., the low  
44 inertia and the predominantly resistive line parameters.

45 For distributed generation (DG) units in three-phase grid-connected systems, two control strategies  
46 are frequently being used in practice. First, the single-phase sinusoidal control strategy is used in case the  
47 three-phase DG unit consists of three single-phase inverters with common dc-bus. Second, a three-phase  
48 control strategy with positive-sequence control can be used. These controllers do not deteriorate the  
49 voltage unbalance, but will not improve it either [7]. Unbalance can be caused, e.g., by asymmetrical  
50 loads, small single-phase DG units or an asymmetrical impedance of the system. The unbalance can  
51 be quantified by means of an unbalance factor, e.g., the voltage unbalance factor (VUF). International  
52 standards, such as EN-50160, pose limits for the VUF as unbalance may lead to adverse effects. They  
53 may evoke additional losses in the electric power system [7]. Also, the negative sequence components  
54 lead to inversely rotating fields, which are hazardous for rotating machines. Further, the capacity of  
55 the grid assets is reduced as the capacity of the transformers or network lines is based on the maximum  
56 current. Compensation of unbalance is usually done by installing dedicated unbalance mitigation devices,  
57 such as active power filters injecting negative sequence voltages or currents [8]. The power quality of the  
58 system can also be improved by adding active power filtering functions in the control strategies of DG  
59 units [9].

60 Like in grid-connected networks, care should be taken to unbalance in islanded microgrids. Many of  
61 the three-phase controllers operate in the  $\alpha\beta$  reference system, where proportional resonant controllers  
62 can be used and the values are transformed back to the stationary reference frame [10], generally  
63 without taking into account unbalance. In extension, inverter-based three-phase DG units can provide  
64 unbalance suppression by using a coordinated algorithm [11,12]. In [13,14], the DG units inject a  
65 negative sequence current of which the negative sequence conductance is controlled in order to reduce the  
66 voltage unbalance. The method is implemented in the synchronous  $dq$  reference frame. The conductance  
67 defined in [14] is determined by a droop characteristic using the negative sequence reactive power. In  
68 this way, the compensation effort is shared between the DG units without inter-unit communication. A  
69 cascaded control loop is used and the compensation term is injected at the input of the inner current  
70 control loop, which equals the output of the outer voltage control loop. It is, thus, considered as a  
71 disturbance for the voltage controller, leading to a trade-off between voltage regulation adequacy and  
72 unbalance compensation efficiency [15]. The voltage unbalance compensation can also be included  
73 directly at the input of the voltage control loop, such as the method in [15] for unbalance compensation  
74 reducing the negative sequence voltage, which is implemented in the stationary  $\alpha\beta$  reference frame.  
75 Compensation of the negative sequence current of unbalanced loads while focusing on minimal negative  
76 sequence currents in the lines is in the scope of [16]. The negative sequence current is shared among the  
77 DG units by adjusting the negative sequence output impedance.

78 In [17], a communication-based controller is added to the droop controller for improving the  
79 voltage quality of a critical load, i.e., compensation of the voltage unbalance and the harmonics. This  
80 compensation effort is shared among the DG units according to their rated powers.

81 This paper has two main aspects. First, the VBD control is extended for three-phase application and  
82 an additional control loop, characterized by the distortion damping resistance  $R_d$ , is included for taking  
83 into account the unbalance in the system. Next, the effect of the value of  $R_d$  is studied. For different  $R_d$ ,  
84 the sharing of unbalance between the DG units and the unbalance mitigation are considered. Unbalance  
85 mitigation can either relate to voltage unbalance near the loads, which leads to adverse effects in load  
86 equipment and more heating and losses in the loads, as well as to current unbalance in the lines, which  
87 evokes increased line losses. The additional control loop in the VBD control is based on a similar strategy  
88 for grid-connected, i.e., grid-following, DG units described in § 2. In § 3, first, the three-phase VBD  
89 control, operating in the stationary  $abc$  reference frame, is presented. Next, the method for unbalance  
90 mitigation in grid-following units (§ 2) is altered for application in the grid-forming DG units and added  
91 to the VBD control as an additional control loop. The effect of the value of distortion damping resistance  
92 is discussed in § 4. In § 5, several case studies to verify the adequacy of the controllers and the effect of  
93 the value of the distortion damping resistance are presented.

## 94 2. Single phase PR-SHI method in grid-connected microgrids

DG units are mostly converter-connected to the distribution network. This offers the opportunity  
for the DG units to provide ancillary services to the electric power system, such as power quality  
improvement. In [9], the power quality is improved by adding active power filtering functions to the DG  
units' control. This control strategy is called the Programmable Resistance Shunt Harmonic Impedance

method (the PR-SHI method) and is used in single-phase DG units. The amount of voltage waveform improvement that can be obtained by one unit is limited with this approach, but the total improvement can be significant because of the large number of DG units [9]. The PR-SHI method determines the inverter's reference current in order to achieve a controlled resistive behavior towards voltage disturbances. This reference injected current  $i_L^*(t)$  constitutes of two components:

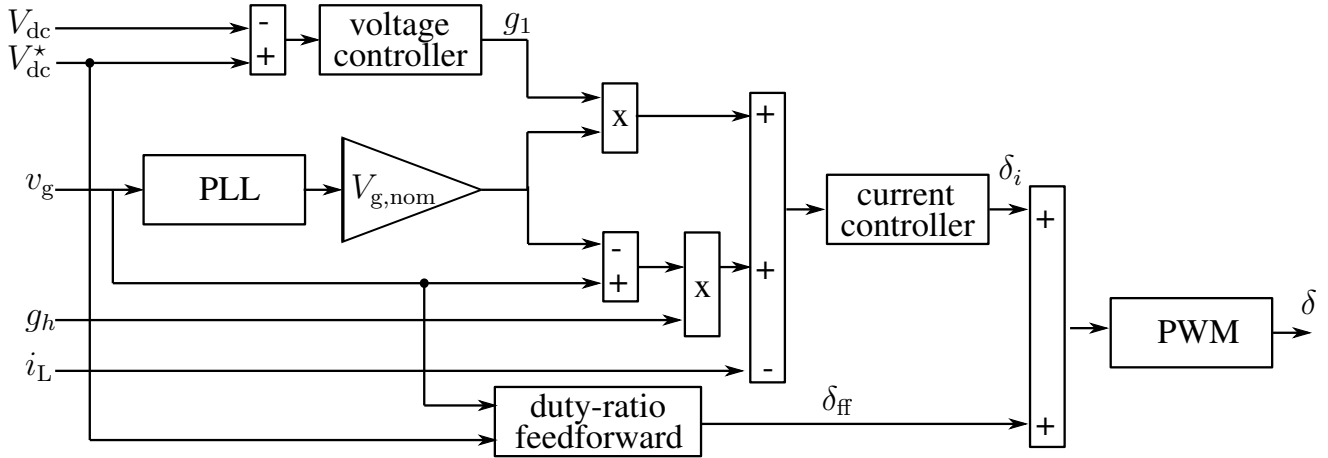
$$i_L^* = g_1 V_{g,\text{nom}} \sin \theta_{\text{PLL}} + g_d (v_g - V_{g,\text{nom}} \sin \theta_{\text{PLL}}), \quad (1)$$

95 with  $V_{g,\text{nom}}$  the nominal amplitude of the grid voltage  $v_g$ ,  $g_1$  the fundamental conductance ( $\Omega^{-1}$ ) and  
 96  $g_d$  the distortion damping conductance ( $\Omega^{-1}$ ). The phase angle  $\theta_{\text{PLL}}$  of the sinusoidal reference signal  
 97 is locked to the phase of the fundamental component of the mains voltage by using a phase-locked  
 98 loop (PLL). The first component in (1) represents the fundamental component to inject a predefined  
 99 amount of power in the network, e.g., the maximum power point of the primary energy source. The  
 100 conductance  $g_1$  is adapted by the dc-link voltage controller to obtain a constant dc-link voltage  $V_{\text{dc}}$ ,  
 101 enforcing that the generated dc-power is equal to the ac power delivered to the electrical network. The  
 102 second term reacts on every deviation of  $v_g$  from its nominal value  $V_{g,\text{nom}} \sin \theta_{\text{PLL}}$ . Hence, this term is  
 103 proportional with the voltage distortion in order to obtain a resistive behavior towards voltage harmonics  
 104 and other voltage distortions such as dips [18]. The control strategy is summarized in Fig. 1. The PR-  
 105 SHI control strategy allows the setting of the distortion damping input conductance ( $g_d^{-1}$ ) independently  
 106 of the fundamental input impedance, and thus, independently of the power level of the converter [18,  
 107 19]. Hence, the converter is able to maintain its damping potential over a wide range of power levels.  
 108 This PR-SHI method is promising because it may swiftly extract the distorted voltage, and also, the  
 109 two components in the injected current are easy both to interpret and to implement in practice. The  
 110 benefits of this control strategy have been discussed in [18,20,21]. This method is extended for three-  
 111 phase application in [7]. Damping the harmonic distortion and voltage dips in single-phase systems and  
 112 unbalance mitigation in three-phase applications have been considered.

113 In conclusion, the factor  $g_h$  damps the deviation of the terminal grid voltage from its ideal value, i.e.,  
 114 due to harmonics and voltage dips. The main advantages of this method are the simplicity to implement  
 115 and the low computational burden. In this paper, this idea is reformed for unbalance mitigation in  
 116 islanded microgrids.

### 117 3. Extension of VBD control to three-phase control, including unbalance mitigation/sharing control 118 loop

119 Current-controlled (i.e., grid-following) three-phase inverters with positive sequence control form an  
 120 open circuit for unbalance in the three-phase system. The grid-forming (i.e., voltage-controlled) inverters  
 121 in islanded systems with positive sequence control on the other hand, form a short-circuit for unbalance  
 122 in the three-phase system. Hence, the converter that is electrically closest to the source of unbalance will  
 123 be burdened with most of the unbalanced current. By implementing a programmable resistive behavior  
 124 for unbalance, similar with the PR-SHI method, the unbalance in islanded networks can be dealt with  
 125 in a controlled manner. Two methods for this are discussed in this paper, namely a method making  
 126 the converter Resistive for Unbalance (RU) versus a method that Contributes in the Weakest phase

**Figure 1.** PR-SHI method for grid-connected DG units

127 (CW). These are both included in the Conventional voltage-based droop (VBD) control Method, i.e.,  
 128 Conventional Method (CM).

### 129 3.1. Extension to three-phase systems

The VBD control method has originally been developed for single-phase systems [6] and is here extended for its three-phase application. The  $V_g/V_{dc}$  droop controller determines the terminal voltage amplitude  $V_g$  of the DG unit based on a measurement of the dc-link voltage  $V_{dc}$ . The  $Q/f$  droop controller determines the phase angle of phase  $a$  ( $\theta_a$ ) based on a measurement of the reactive power output of the unit. In the CM, the phase angles of the other phases are determined by a phase-shifting this voltage with  $2\pi/3$ , hence, the CM does not take into account the unbalance in the microgrid. The three phases inject a voltage with the same amplitude  $V_g$ . In this way, a direct voltage component is generated. Together, these digital controllers determine the reference voltage  $v_{\text{droop},i,k}^* = V_{g,k} \sin(\theta_{i,k})$  ( $k$  is the discrete time instance and phase  $i = a, b, c$ ). Discrete values are utilized because pulse width modulation with sampling period  $T_s$  is used in the converter:

$$v_{\text{droop},i,k}^* = V_{g,k} \sin(\theta_{i,k-1} + 2\pi f_k T_s), \quad (2)$$

130 with  $f_k$  the frequency at discrete time instant  $k$ , which is determined by the  $Q/f$  droop controller. Hence,  
 131 the grid-forming VBD control determines the reference value  $v_{\text{ref},i}^*$  of the output voltage of the DG unit.  
 132 In the Conventional Method,  $v_{\text{ref},i}^* = v_{\text{droop},i}^*$ . From the measurement of  $V_{dc}$ , the  $V_g/V_{dc}$  droop controller  
 133 determines the reference amplitude of the grid voltage  $V_g$ . Hence, in the CM, this value is equal for all  
 134 three phases. In an unbalanced grid, the output currents of the DG unit can be unbalanced, the voltage is  
 135 balanced because it is a controlled value in the grid-forming DG units.

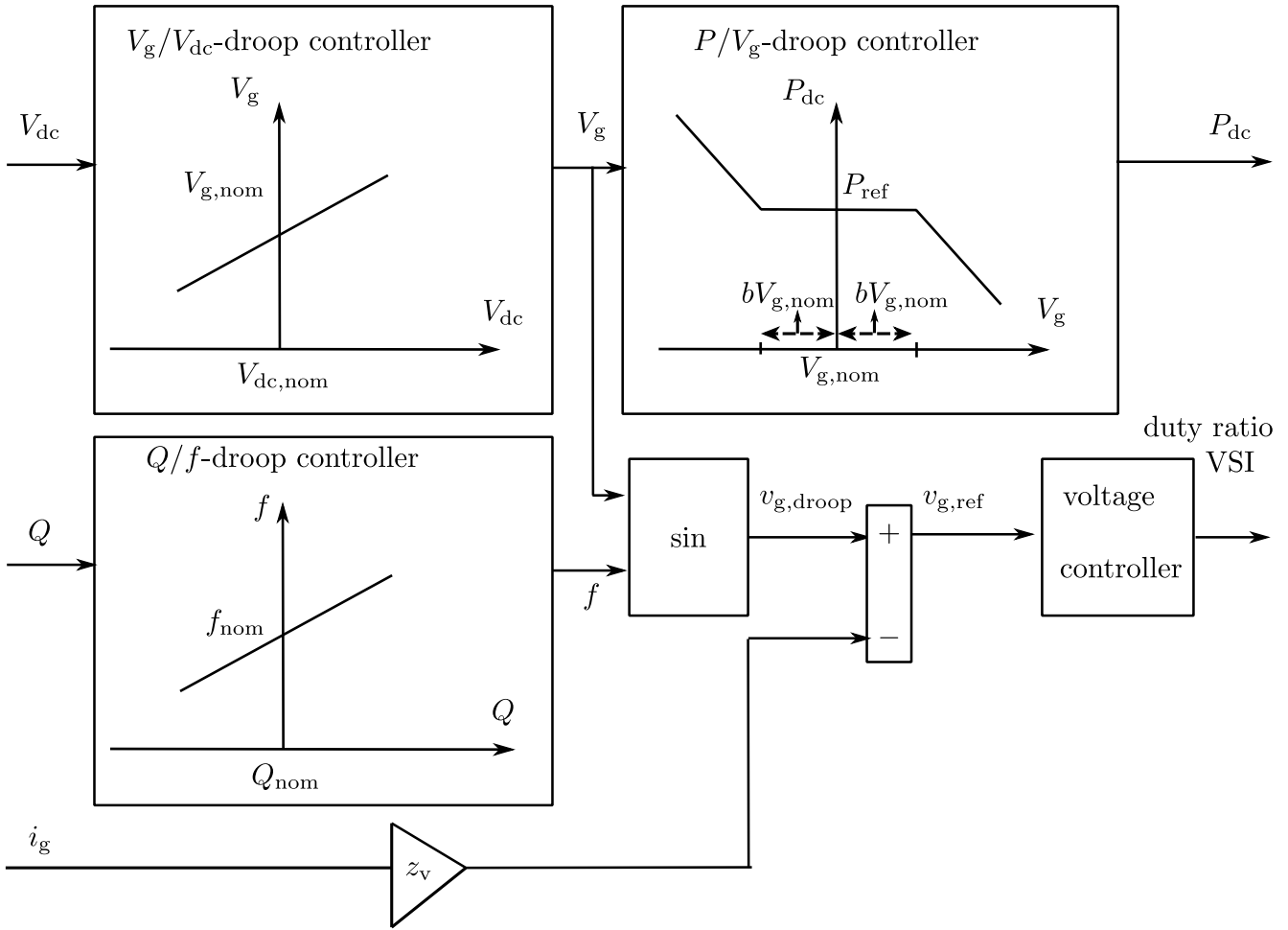
**Figure 2.** VBD controller and virtual impedance loop

Fig. 2 shows the VBD control strategy including a virtual output impedance loop. A resistive output impedance  $z_v = R_v$  is chosen as this provides more damping in the system [22] and complies with the power control strategies of the loads and generators:

$$v_{\text{ref},i,k}^* = v_{\text{droop},i,k}^* - R_v i_{g,i,k}, \quad (3)$$

136 with  $v_{\text{ref},i,k}^*$  the reference voltage for the voltage controller,  $v_{\text{droop},i,k}^*$  the voltage obtained by the VBD  
 137 controller and  $i_{g,i,k}$  the grid current delivered by the DG unit in phase  $i$ . The VBD controller also  
 138 determines the input power  $P_{\text{dc}}$  of the unit by means of a  $P_{\text{dc}}/V_g$  droop controller. A constant-power  
 139 band with width  $2bV_{g,\text{nom}}$  is included in the latter controller. By determining the value of  $b$  according to  
 140 the characteristics of the energy source, priority of active power injection is automatically set between  
 141 different DG units. Less dispatchable DG units (e.g., combined heat and power (CHP) units) have a  
 142 larger constant power band than dispatchable units (e.g., diesel generators).

143 **3.2. Additional of voltage unbalance control loop**

In the RU and CW method, an additional control loop is included such that the DG units have a resistive behavior towards current distortions:

$$v_{\text{ref},i}^* = v_{\text{droop},i}^* - R_v i_{g,i} - R_d (i_{g,i} - i_{\text{balanced},i}), \quad (4)$$

with  $i_{\text{balanced},i}$ , the ideal grid current as defined below and  $R_d$  the distortion damping resistance. The theoretically balanced grid current provided by the DG unit equals:

$$i_{\text{balanced},a} = \frac{\sqrt{2}}{3} \frac{\sqrt{Q^2 + P^2}}{V_g/\sqrt{2}} \sin(\arctan \frac{Q}{P_{\text{dc}}} + \theta_a), \quad (5)$$

with  $\theta_a$  the phase angle of the voltage reference determined by the  $Q/f$  droop controller.  $Q$  and  $P$  are the measured total reactive and active power output of the DG unit.  $P_{\text{dc}}$  is the output variable of the  $P_{\text{dc}}/V_g$  droop controller, in steady state,  $P_{\text{dc}} = P$ . The balanced current of phase b is determined analogously:

$$i_{\text{balanced},b} = \frac{\sqrt{2}}{3} \frac{\sqrt{Q^2 + P^2}}{V_g/\sqrt{2}} \sin(\arctan \frac{Q}{P_{\text{dc}}} + \theta_b) \quad (6)$$

144 with  $\theta_b = \theta_a - \frac{2\pi}{3}$  and similarly for  $\theta_c$ . In the CM,  $R_d = 0\Omega$ , in the RU method  $R_d > 0\Omega$  and in  
 145 the CW method  $R_d < 0\Omega$ . Eq. (4) is the grid-forming variant of the PR-SHI method which provides a  
 146 resistive behavior of the grid-following unit towards voltage distortions. With grid-forming controllers,  
 147 only action towards current distortions can be taken in a straightforward manner because the units are  
 148 voltage-controlled.

#### 149 4. Value of the distortion damping resistance $R_d$ : qualitative study

150 In this section, the effect of choosing a positive versus negative value of  $R_d$  on the unbalance  
 151 mitigation, the power sharing between phases in a DG unit and the line losses in the microgrid is  
 152 discussed in a qualitative manner. In section 5, this will further be quantitatively verified by means  
 153 of simulations.

In this paragraph, the voltage unbalance factors of the different methods, i.e., CM, RU and CW methods, will be compared. The voltage unbalance factor (VUF) equals

$$\text{VUF} = V_2/V_1 \quad (7)$$

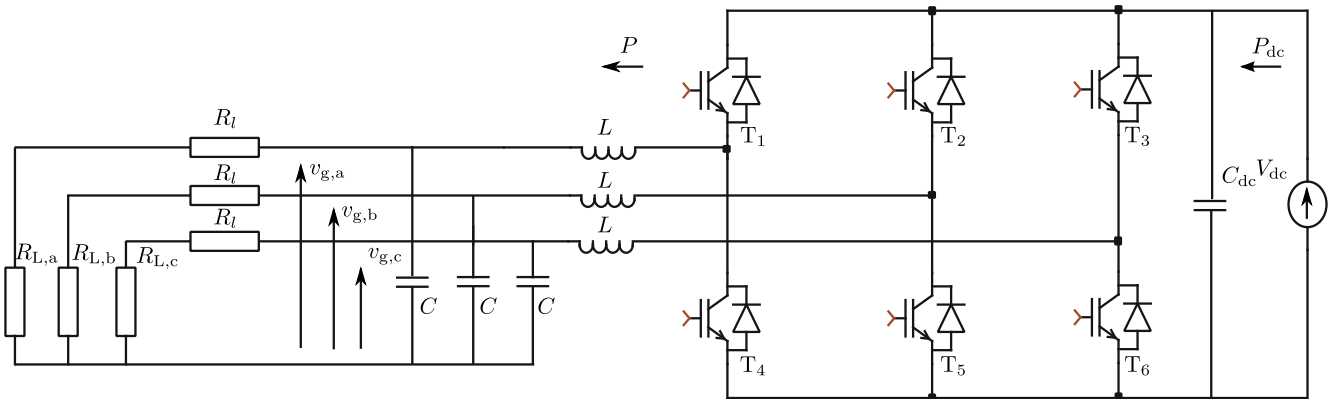
with  $V_2$  the inverse and  $V_1$  the direct component of the three-phase signal  $V$  (consisting of the  $V_a$ ,  $V_b$  and  $V_c$  components):

$$\begin{bmatrix} V_0 \\ V_1 \\ V_2 \end{bmatrix} = \frac{1}{3} \begin{bmatrix} 1 & 1 & 1 \\ 1 & a & a^2 \\ 1 & a^2 & a \end{bmatrix} \begin{bmatrix} V_a \\ V_b \\ V_c \end{bmatrix} \quad (8)$$

The current unbalance factor (CUF) is calculated analogously, with  $I$  the current:

$$\text{CUF} = I_2/I_1 \quad (9)$$



**Figure 3.** Islanded microgrid with three-phase inverter

#### 154 4.1. Islanded microgrid: one DG unit

155 The difference between the RU ( $R_d > 0$ ) and CW method ( $R_d < 0$ ) is discussed in this section.

156 For this purpose, one DG unit and an unbalanced load with a larger load in phase a than in the phases  
 157 b and c are considered in an islanded microgrid depicted in Fig. 3 ( $R_{L,a} < R_{L,b/c}$ ). The three-phase DG  
 158 unit utilizes VBD control with  $b = 8\%$  and  $R_v = 0\Omega$  including a distortion damping with factor  $R_d$ , to  
 159 determine the reference voltage.

160 With the conventional VBD control method (CM), the three reference voltages have an equal  
 161 amplitude and a 120 degrees phase shift in case  $R_v = 0\Omega$ . Hence, in the considered network, the current  
 162  $i_a$  will be higher than  $i_b$  and  $i_c$ .

163 In the CW variant, the current  $i_a$  will be even larger because of the additional contribution in the  
 164 weakest phase a. In this case, the VUF at the load terminals will, thus, be lower than in the CM  
 165 case (higher  $i_a$  combined with lower  $R_a$ ). This lower unbalance factor is beneficial for, e.g., induction  
 166 machines. However, for the same amount of delivered active power, the line losses will be significantly  
 167 larger as the current unbalance factor CUF of the current in the lines is higher. The VUF at the DG unit  
 168 terminals will be higher than in the CM case. In summary, the CW variant is beneficial for the VUF near  
 169 the loads. It is disadvantageous for the VUF of the DG unit's terminal voltage and the CUF, hence for  
 170 line losses in the microgrid. Also, the loading is more unevenly spread over the three phases of the DG  
 171 unit than in the CM.

172 In the RU variant, the current  $i_a$  will be lower than in the CM. Hence, the loading of the DG unit will  
 173 be more evenly shared between its three phases. Subsequently, the DG unit can inject more power in the  
 174 grid without increasing the ratings of its inverter. The RU variant is good for the CUF in the lines, hence  
 175 for the line losses. However, the VUF near the load will be higher than in the CM and CW case.

176 An overview of the advantages and disadvantages of the three methods is given in Table 1. The choice  
 177 between RU and CW is dependent on the objectives in case a single DG unit is considered. Note that the  
 178 RU method adds damping to the system (resistive behavior), while for the CW method, careful attention  
 179 should be paid to the microgrid stability. For this, root locus analysis is often used, such as [23].

#### 180 4.2. Grid-connected microgrid, one DG unit



**Table 1.** Islanded microgrid, one DG unit

	RU method	CW method	CM
current unbalance, line losses	+	-	0
voltage unbalance of load	-	+	0
equalization of power in phases of DG	+	-	0
voltage unbalance of DG units	-	-	+

181 In the grid-connected case with grid-forming control strategy of the DG units (which has the  
 182 advantage that the same controller can be used both in grid-connected and islanded mode), the CW  
 183 method supports the weakest phase. Subsequently, the utility network can provide a more balanced  
 184 current. This is beneficial for the utility network as the unbalance remains local, inside the microgrid  
 185 (Table 2). The RU method achieves a more balanced current in the section between the DG unit and the  
 186 load. However, as the VUF at the DG unit's and load's terminal voltages are higher, the utility needs  
 187 to deliver a more unbalanced current. The effect on the losses in the microgrid depends thus on the  
 188 configuration.

**Table 2.** Grid-connected microgrid, one DG unit

	RU method	CW method	CM
current unbalance of grid current	-	+	0

### 189 4.3. Islanded microgrid: unbalance sharing

190 For analysis of the sharing of unbalance between multiple DG units, a simple islanded microgrid  
 191 consisting of two DG units and an unbalanced load is considered. In the CM, both DG units deliver a  
 192 balanced voltage, hence, most of the unbalanced current needs to be provided by the DG unit that is  
 193 electrically closest to the unbalanced load. Hence, this unbalance sharing is not actively controlled. By  
 194 properly setting the parameter  $R_d$ , the sharing between the DG units can be altered. The unit with the  
 195 lower  $R_d$  will be burdened with most of the unbalance. The effect on the CUF and the VUF depends on  
 196 the configuration of the microgrid and the chosen  $R_d$  values.

197 For comparing the three methods, Table 1 remains valid. By lowering the  $R_d$  of one DG unit, this unit  
 198 will contribute more in feeding the unbalance, compared to the DG unit with high  $R_d$  which will deliver  
 199 less of the unbalance.

### 200 4.4. Discussion

201 In grid-connected mode, the CW variant is generally most beneficial from the utilities point of view. In  
 202 the islanded mode with one grid-forming DG unit, the choice between the CW and RU methods depends  
 203 on the goals set. Generally, the unbalance factor near the loads is most important, leading to the CW  
 204 variant as best option. However, the RU variant achieves less line losses and a more even power sharing  
 205 between the three phases of the DG unit, leading to less overrating of this unit. As will be shown further,

206 the RU variant, providing a positive resistance, includes additional damping in the system. Therefore, in  
207 case multiple DG units in islanded microgrids are considered, the RU method is generally most effective  
208 for this stability reason. Both the RU and CW methods enable in actively influencing the unbalance  
209 sharing between different DG units.

## 210 5. Value of the distortion damping resistance $R_d$ : simulation study

211 In the previous section, a qualitative comparison between the three methods,  $R_d = 0\Omega$ ,  $R_d > 0\Omega$  and  
212  $R_d < 0\Omega$  is given. When tuning the exact value of  $R_d$ , one should take into account the line resistance  
213 of the grid (here low-voltage, thus mainly resistive, microgrids are considered). Generally, a good value  
214 of  $R_d$  is one in the same order of magnitude as the line resistance in case of urban grids. In case of rural  
215 grids, the effect of the unbalance sharing is sufficiently clear if the value of  $R_d$  is in the same order of  
216 magnitude as the virtual resistance  $R_v$ , which generally is approximately equal to a few times the value  
217 of the line resistance  $R_l$ . Generally, no  $R_v$  is required if  $R_l > 1\Omega$  (rural grids), while the control loop  
218 with  $R_v$  is included when  $R_l < 1\Omega$  (urban grids). Only in case multiple DG units are considered and the  
219 contribution of the provision of unbalance is to be determined, it is more important to take into account  
220 all DG units for tuning the values of  $R_d$ .

221 In this section, the three theoretical cases described above are analyzed. First, an islanded microgrid  
222 with one DG unit is considered (see § 4.1). The CM, CW and RU methods are compared. Next, a  
223 grid-connected microgrid is briefly discussed (see § 4.2). Third, the unbalance sharing between multiple  
224 DG units in islanded mode is considered (see § 4.3). Finally, a dynamic simulation is included.

### 225 5.1. Islanded microgrid, one DG unit

226 In this case, the islanded microgrid of Fig. 3 as described above is considered. Purely resistive line  
227 parameters  $R_l$  are assumed as low-voltage networks are studied [5,24]<sup>1</sup>. In [25], it is concluded that the  
228 effect of a realistic R/X on the VBD control is limited, even more so when including virtual resistance  
229 in the microgrid lines as the real R/X seen by the DG units becomes  $((R+R_v)/X)$ . For these reasons, this  
230 is not considered in this paper, purely line resistances are assumed, i.e.,  $R + R_v$  is sufficiently larger  
231 than  $X$ . The load is a grounded star-connection of  $20\Omega$  in phase a and  $400\Omega$  in phases b and c. The  
232 nominal power of the DG unit equals 2500 W, the unit has a constant-power band  $b$  of 8 %, representing  
233 a slightly dispatchable DG unit. Small-scale microgrids are often burdened with even more unbalance  
234 problems compared to the conventional networks because the small amount of single phase loads balance  
235 each other out only a little bit when there are a small number of loads. Hence, in the simulations, the  
236 unbalance is exaggerated such that the unbalance mitigation becomes stringent. First, a rural network  
237 is considered, generally characterized by long lines. This allows for applying the VBD control without  
238 virtual resistance. The advantage of the latter is that the separate effect of  $R_v$  and  $R_d$  can be studied.

---

<sup>1</sup> In purely resistive networks, the active power is linked with the grid voltage, while in inductive networks, a well known reactive power/grid voltage linkage exists. Generally, the R/X value in low-voltage microgrids is sufficiently high, such that the voltage is predominantly linked with the active power.

**Table 3.** One DG unit: CM (conventional method) versus RU versus CW variant ( $R_l = 3 \Omega$  and  $R_v = 0 \Omega$ )

Parameter method	$R_d = 0$ CM	$R_d = -3 \Omega$ CW	$R_d = 3 \Omega$ RU
$P_a$ (W)	2244	2299	2186
$P_b, P_c$ (W)	128	101	157
$V_{g,a}$ (V)	227.2	229.9	224.2
$V_{g,b}, V_{g,c}$ (V)	227.2	201.4	251.6
VUF( $v_g$ )	0	0.0450	0.0376
CUF( $i_g$ )	0.8463	0.8636	0.8297
VUF( $v_L$ )	0.0431	0	0.0788
losses (W)	295	301	287

239 Next, a more urban low-voltage microgrid is considered, where also virtual resistance is included. The  
 240 separated effect of virtual and damping resistances becomes less clear but the same conclusions are valid.

#### 241 5.1.1. Without $R_v$

242 Table 3 shows the simulation results for the case of a relatively large line resistance  $R_l$ , i.e., a rural  
 243 network, and, hence, without virtual resistance  $R_v$ . All three methods obtain a stable microgrid operation.  
 244 As the voltage is close to the nominal voltage (in the  $\pm 8\%$  voltage band), the delivered power of the  
 245 DG unit equals 2.5 kW in all three cases. In the conventional method (CM), the DG unit, which is  
 246 grid-forming, thus voltage-controlled, generates a balanced output voltage. Hence, the VUF( $v_g$ ) is equal  
 247 to zero 0. Therefore, the line current is largely unbalanced, acquiring a large CUF( $i_g$ ).

248 The RU method shows a resistive behavior towards unbalanced currents, hence, it generates some  
 249 unbalance in the terminal voltage of the DG units (VUF( $v_g$ ) > 0) to counteract the unbalance in the  
 250 line currents CUF( $i_g$ ). Consequently, the line losses are lower. Also, the 2.5 kW output power is more  
 251 evenly spread among the three phases of the DG unit, which is beneficial, first for the inverter losses  
 252 which depend on the current amplitude and second, from a planning perspective as the same amount of  
 253 power can be delivered with a lower rating of the DG unit. A disadvantage is that the voltage unbalance  
 254 near the load, thus the VUF( $v_L$ ), has increased.

255 The CW method lowers the VUF of the load, with the cost of increased unbalance in the line currents  
 256 and subsequently, larger line losses. Also, the power is less evenly spread between the three phases of  
 257 the DG unit, as illustrated in Table 3.

#### 258 5.1.2. With $R_v$

259 In table 4, resistive virtual impedance is added to the system to provide more damping when facing  
 260 a lower line resistance, e.g., in urban microgrids with lower line resistance. The primary effect of adding  
 261  $R_v \neq 0$  is that also in the CM, the VUF( $v_g$ ) becomes a nonzero value. The table again shows that the  
 262 CW method supports the weakest phase, which increases the unbalance in the output power of the DG  
 263 unit. The VUF of the load is better in the CW method than in the RU case, but at the expense of more  
 264 line losses.

**Table 4.** One DG unit: RM (conventional method) versus RU versus CW variant ( $R_l = 0.3 \Omega$  and  $R_v = 1.5 \Omega$ )

Parameter method	$R_d = 0$ CM	$R_d = -3 \Omega$ CW	$R_d = 3 \Omega$ RU
$P_a$ (W)	2240	2299	2178
$P_b, P_c$ (W)	130	101	161
VUF( $v_g$ )	0.0223	0.0246	0.0609
CUF( $i_g$ )	0.8532	0.8708	0.8369
VUF( $v_L$ )	0.0268	0.0198	0.0653
losses (W)	33.3	34.1	32.4

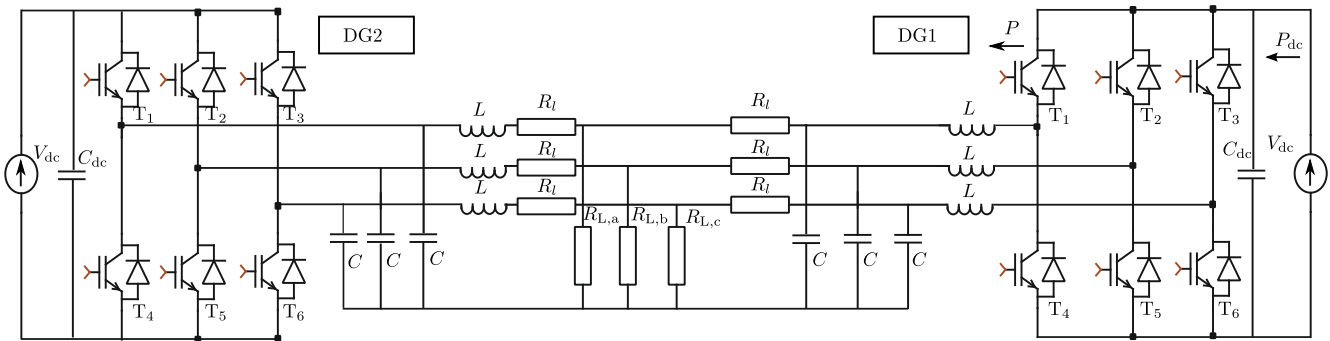
265 The effect of including a resistive virtual output impedance  $R_v$  in the VBD control is that it provides  
 266 additional damping in order to acquire a stable system operation despite the low line resistances. Such  
 267 low  $R_l$  indeed implies that a low voltage change could lead to a relatively large variation in the power  
 268 flow, which makes the system difficult to stabilize.

### 269 5.1.3. Discussion

270 In this paragraph, the theoretical statements of § 4.1 are validated. Without additional control loops,  
 271 the conventional VBD control method, i.e., CM, can achieve a stable three-phase microgrid operation  
 272 but the unbalance cannot be actively handled. A positive distortion damping resistance  $R_d$  in the RU  
 273 method emulates a resistive behavior of the DG unit towards unbalance, lower current imbalance in the  
 274 lines and hence, lower line losses. Also, the RU method spreads the output power more evenly over the  
 275 three phases of the DG unit, at the expense of larger VUF of the load. A negative  $R_d$  in the CW method  
 276 better mitigates the voltage unbalance of the loads, at the expense of larger line losses and the output  
 277 power of the DG unit being more unevenly spread between the three phases, which was also expected in  
 278 §4.1, see Table 1.

279 *5.2. Grid-connected microgrid, one DG unit* In this paragraph, following § 4.2, a grid-connected  
 280 microgrid is studied. From a theoretical point of view, the goals of the unbalance mitigation scheme is to  
 281 mitigate the unbalance seen by the utility grid, opposed to the case in § 4.1 and 5.1. The here-considered  
 282 microgrid consists of the same grid as previously, with the load connected to a three-phase utility grid.  
 283 The grid is modeled as a strong three-phase balanced voltage source generating a 50 Hz phase voltage  
 284 of 230 V rms. The microgrid topology is depicted in Fig. 4, but with the three-phase grid as described  
 285 above instead of DG2. The DG unit's nominal power equals 2.5 kW, and it has a constant-power band of  
 286 8 %. The advantage of using the VBD control strategy, both RU, CW and CM, is that the microgrid can  
 287 be controlled with the same control strategy in islanded and grid-connected mode [26].

288 Table 5 shows that the CW method supports the grid which has to deliver less of the unbalanced power  
 289 as the DG units inject more power in the phase with the largest load. Subsequently, lower line losses are  
 290 obtained in the line segment between the utility and the load. The load voltage is better balanced at the

**Figure 4.** Islanded microgrid with two three-phase inverters**Table 5.** Grid-connected microgrid and one DG unit: RM (conventional method) versus RU versus CW variant (Rural:  $R_l = 3 \Omega$ ,  $R_{grid} = 2 \Omega$ ,  $R_v = 0 \Omega$ )

Parameter method	$R_d = 0$	$R_d = -3 \Omega$	$R_d = 3 \Omega$
	CM	CW	RU
$P_a$ (W)	1500	2695	1224
$P_b, P_c$ (W)	500	-98	638
VUF( $v_g$ )	0	0.0456	0.0108
CUF( $i_g$ ) - DG unit	0.3996	1.1355	0.2461
CUF( $i_n$ ) - grid	0.7894	0.6357	0.8675
VUF( $v_L$ )	0.0183	0	0.0226
losses (W) L to DG	144	326	124
losses (W) U to L	27.3	3.1	41.1

291 expense of higher CUF in the grid current injected by the DG unit, hence, larger line losses in the section  
 292 between load and DG unit.

293 The adverse VUF of the load is a cost to be paid with positive  $R_d$  for lowering the line losses in the  
 294 segment between the DG unit and the load and improving the DG unit's operation (more even distribution  
 295 of output power between phases). In the RU method, the unbalanced currents are to a large extent  
 296 delivered by the utility network (CUF( $i_n$ )). In the CW method, these are provided by the DG unit inside  
 297 the microgrid. From the utilities point of view, this is a significant benefit as the microgrid can be regarded  
 298 as a controllable entity mitigating current unbalance. Vice versa, the adverse CUF of the DG units output  
 299 currents (CUF( $i_g$ )) and increased ratings is a cost to be paid with negative  $R_d$  for improving the voltage  
 300 unbalance near the loads and mitigating the unbalance of the utility.

301 **5.3. Islanded microgrid, unbalance sharing** In this paragraph, the unbalance sharing between multiple

302 DG units in an islanded microgrid is considered. First, a symmetrical microgrid is considered. The  
 303 CM, CW and RU methods are compared in Tables 6 and 7. Only two DG units are considered, but  
 304 the conclusions can be extrapolated for multiple units. Second, it is shown that by choosing a proper  
 305 distortion damping resistance  $R_d$ , the unbalance sharing between DG units can be actively controlled in  
 306 Table 8. Third, an asymmetrical microgrid is studied in Tables 9 to 10 in order to illustrate that with the  
 307 CM, the microgrid configuration determines the unbalance sharing whereas the CW and RU methods

**Table 6.** Islanded microgrid with two DG units: CM versus RU versus CW variant ( $R_l = 3 \Omega$ ,  $R_v = 0 \Omega$ ) - I

Parameter	$R_d = 0$ DG 1 and 2	$R_d = 3\Omega$ DG 1 and 2	$R_d = -3\Omega$ unstable
$P_a$ (W)	2364	2282	
$P_b, P_c$ (W)	68	84	
$V_{g,a}$ (V)	233.1	229.1	
$V_{g,b}, V_{g,c}$ (V)	233.1	258.0	
VUF( $v_g$ )	0	0.0388	
CUF( $i_g$ )	0.9124	0.9063	
VUF( $v_L$ )	0.0443	0.0811	
losses (W)	310.3	298.8	

308 achieve an active control of this. Fourth, in Table 11, DG units of different ratings are included, showing  
 309 that a proper setting of  $R_d$  according to the units' ratings allows for a better sharing of the unbalance.

310 For analyzing the unbalance sharing, an islanded microgrid consisting of two DG units and an  
 311 unbalanced load, as depicted in Fig. 4, is considered. The load has  $10\Omega$  in phase a and  $400\Omega$  in phases  
 312 b and c. Both DG units have a constant-power band of 8 % and have equal ratings  $P_{dc,nom} = 2500$  W,  
 313 except when explicitly stated otherwise. The line impedances between the DG units and the load are  
 314 sufficiently large such that the effects of  $R_v$  and  $R_d$  can be separated. An analysis of a microgrid with  
 315 smaller line impedances is given in Table 4.

### 316 5.3.1. Symmetrical microgrid: comparison CW and RU method

317 In the first case, a symmetrical line configuration is considered i.e.,  $R_{l,1} = R_{l,2}$ . Also, the DG units  
 318 are symmetrical, i.e., equal ratings and equal parameters. The two DG units give equal results, hence,  
 319 the tables only show the results of one unit.

320 Table 6 compares the CM, CW and RU methods in this symmetrical microgrid. The RU method  
 321 clearly achieves lower line losses and a better balancing of the output current between the three phases  
 322 compared with the CM. However, the VUF of the load is worse. The CW method proves to be unstable  
 323 in this case as a negative  $R_d$  lowers the damping of the system.

324 In table 7, exactly the same configuration is considered, but with a lower  $R_d$ . Clearly the RU method  
 325 with low  $R_d$  achieves less of the valued benefits compared to having a large  $R_d$ , i.e., line loss reduction  
 326 and equalizing of the DG unit's output power between the phases. However, the VUF at the load terminals  
 327 is better. The choice of  $R_d$  hence provides a trade-off between unbalance in the grid currents and in the  
 328 load voltage. The CW method is stable in this case. It achieves a better voltage unbalance mitigation of  
 329 the load with the cost of increased line losses.

### 330 5.3.2. Symmetrical microgrid configuration: affecting unbalance sharing by setting different $R_d$

331 In this paragraph, the effect of setting different  $R_d$  in the DG units in order to affect their contribution  
 332 in the unbalance sharing is studied.

**Table 7.** Islanded microgrid with two DG units: RU versus CW variant ( $R_l = 3 \Omega$ ,  $R_v = 0 \Omega$ )  
- II

Parameter	$R_d = 1 \Omega$	$R_d = -1 \Omega$
	DG 1 and 2	DG 1 and 2
$P_a$ (W)	2353	2373
$P_b, P_c$ (W)	74	64
$V_{g,a}$ (V)	232.6	233.6
$V_{g,b}, V_{g,c}$ (V)	242.4	223.7
VUF( $v_g$ )	0.0137	0.0145
CUF( $i_g$ )	0.9103	0.9095
VUF( $v_L$ )	0.0573	0.0304
losses (W)	308.7	313.2

**Table 8.** Islanded microgrid: power sharing between two DG units with different  $R_d$  ( $R_l = 3 \Omega$ ,  $R_v = 0 \Omega$ )

Parameter	$R_{d,DG1} = 0 \Omega$		$R_{d,DG1} = 0 \Omega$	
	$R_{d,DG2} = 3 \Omega$		$R_{d,DG1} = -3 \Omega$	
	DG 1	DG 2	DG 1	DG 2
$P_a$ (W)	2898	1794	854	3889
$P_b, P_c$ (W)	-201	355	852	-663
VUF( $v_g$ )	0	0.0273	0	0.0934
CUF( $i_g$ )	1.2361	0.5970	0.0286	2.1655
VUF( $v_L$ )	0.0573		0.0019	
losses (W) L to DG	450.4	203.9	151.6	829.4

333 Table 8 shows the case where the  $R_d$  of the two DG units differs, again with  $b = 8\%$ . The first DG  
334 unit does not incorporate the resistive behavior and hence,  $R_{d,DG1} = 0 \Omega$ . The second DG unit utilizes  
335 the RU or CW method. The DG unit with the lowest  $R_d$  will be burdened with most of the unbalance. In  
336 this way, the unbalance sharing can be affected by the control strategy. The choice between positive and  
337 negative  $R_d$  values for all DG units is the same as for the case with one DG unit, taking into account the  
338 lower damping of the system with negative  $R_d$ .

339 In the RU method of the second DG unit, this unit clearly bares less of the unbalance. In the CW  
340 method, this unit bares more of the unbalance and, like in the case of one DG unit, the VUF of the  
341 load has improved with the cost of increased line losses. The unbalance sharing can, thus, effectively be  
342 controlled by choosing a proper value of  $R_d$ .

### 343 5.3.3. Asymmetrical microgrid configuration: : comparison CW and RU method

344 In this paragraph, it is illustrated that the line impedance determines the unbalance sharing in the CM,  
345 whereas with the CW and RU methods, this sharing can be managed by the control strategy. In this case,  
346 the line resistances near the two DG units are different. The results are depicted in Tables 9 and 10. A  
347 resistive virtual impedance is included to add damping in the face of the lower line resistance  $R_l = 0.3 \Omega$ .



**Table 9.** Islanded microgrid: power sharing between two DG units with different  $R_l$ , part 1 ( $R_{l,1} = 0.3 \Omega$ ,  $R_{l,2} = 3 \Omega$ ,  $R_v = 3 \Omega$ )

Parameter	$R_d = 0\Omega$		$R_d = 3\Omega$	
	DG 1	DG 2	DG 1	DG 2
$P_a$ (W)	2620	1806	2151	1734
$P_b, P_c$ (W)	-60	215	52	117
VUF( $v_g$ )	0.0574	0.0290	0.0913	0.0619
CUF( $i_g$ )	1.0574	0.7289	0.9463	0.8475
VUF( $v_L$ )	0.0605		0.0943	
losses (W) L to DG	47.5	192.8	36.8	196.1

**Table 10.** Islanded microgrid: power sharing between two DG units with different  $R_l$ , part 2 ( $R_{l,1} = 0.3 \Omega$ ,  $R_{l,2} = 3 \Omega$ ,  $R_v = 3 \Omega$ )

Parameter	$R_d = -3\Omega$	
	DG 1	DG 2
$P_a$ (W)	3577	1125
$P_b, P_c$ (W)	-539	688
VUF( $v_g$ )	0.0016	0
CUF( $i_g$ )	1.6299	0.1751
VUF( $v_L$ )	0.0089	
losses (W) L to DG	84.6	130.0

348 Table 9 shows that with  $R_d = 0\Omega$ , with the CM, the unit that is electrically closest to the load  
349 (here DG1) bares significantly more of the unbalance. This sharing is thus not actively controlled, but  
350 is determined by the microgrid configuration. The VUF of the DG units' terminal voltage is not zero  
351 because  $R_v$  has a nonzero value. With the RU method, the unbalance is more evenly shared between the  
352 two DG units. The CW method in Table 10 leads to a worse sharing of unbalance, i.e., DG 1 bares even  
353 more of the unbalance, but a better VUF of the load voltage.

#### 354 5.3.4. Symmetrical microgrid configuration: different ratings of DG units

355 In this paragraph, it is shown that the unbalance sharing can be controlled to become according to the  
356 ratings of the DG units.

In this case, the nominal power of the DG units equals 1.6 and 3.2 kW respectively. The results are given in Table 11. Despite the different ratings, the DG units with CM are evenly burdened with the unbalance because of the symmetric microgrid configuration. The inverse components of the delivered grid currents of the two DG units are about equal as

$$\text{CUF}(i_{1,\text{DG1}})/\text{CUF}(i_{1,\text{DG2}}) \approx 2 = P_{\text{nom,DG2}}/P_{\text{nom,DG1}}. \quad (10)$$

**Table 11.** Islanded microgrid: power sharing between two DG units with different ratings ( $R_l = 3 \Omega$ ,  $R_v = 0 \Omega$ )

Parameter	$R_{d,DG1} = 0\Omega$ $R_{d,DG2} = 0\Omega$		$R_{d,DG1} = 2\Omega$ $R_{d,DG2} = 1\Omega$	
	DG 1	DG 2	DG 1	DG 2
$P_a$ (W)	1975	2549	1795	2707
$P_b, P_c$ (W)	-186	324	-97	245
VUF( $v_g$ )	0	0	0.0243	0.0148
CUF( $i_g$ )	1.3296	0.6936	1.1573	0.7764
VUF( $v_L$ )	0.0443		0.0628	
losses (W) L to DG	237.6	377.8	198.9	413.9

357 In the second column of Table 11, the parameter  $R_d$  is set differently for the DG units. This illustrates  
 358 that the setting of  $R_d$  can induce an unbalance sharing which can be actively affected by the control  
 359 strategy.

#### 360 5.4. Dynamic simulation

361 A dynamic simulation with varying load, DG output and distortion damping resistance  $R_d$  is included.  
 362 The microgrid configuration is depicted in Fig. 4.

363 Both DG units are rated at 3.5 kW and have a constant-power band of 8 %. From  $0 < t < 0.8$  s,  
 364  $R_d = 3 \Omega$  for both units and the load is balanced and equal to  $20 \Omega$  in each phase. At  $t = 0.8$  s, the  
 365 load becomes unbalanced as in phase a, an additional  $20 \Omega$  load turns on in parallel with the first one. At  
 366  $t = 1.6$  s, the output of DG1 increases with 1 kW. From  $t = 2.4$  s on, the  $R_d$  of DG1 becomes zero and  
 367 at  $t = 3.2$  s, the output of DG1 drops again to its nominal value. Fig. 5 shows the obtained results.

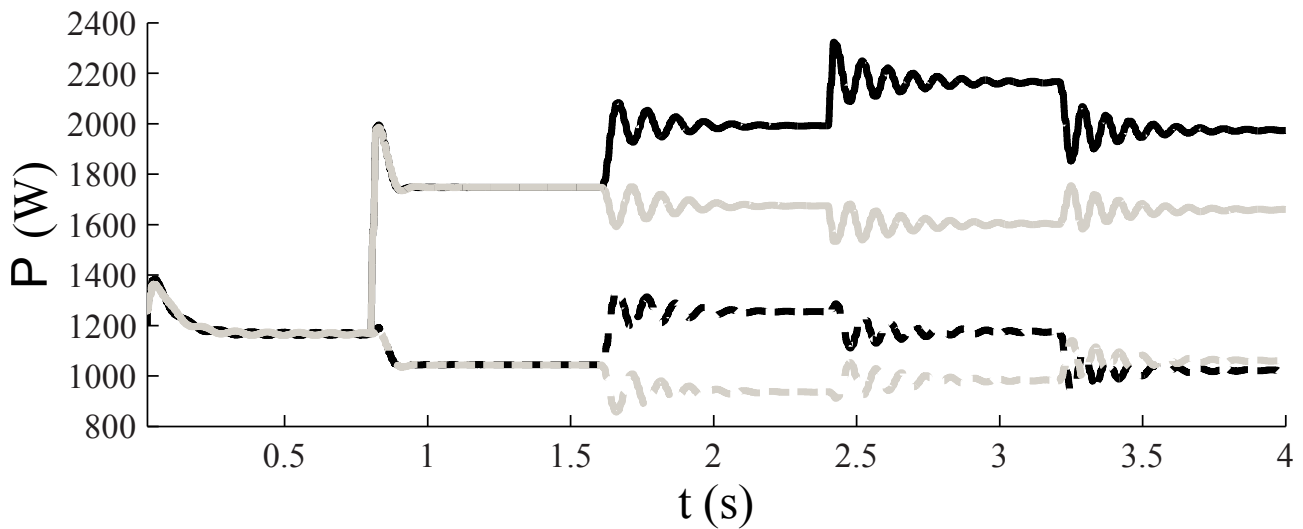
368 In conclusion, a stable three-phase microgrid operation is shown despite the large unbalance in the  
 369 system. Relatively small transients are obtained despite the large variations in the small-scale islanded  
 370 microgrid. After the  $R_d$  decrease (after 2.4s) in DG1, this unit is clearly more burdened with the delivery  
 371 of unbalanced currents. Hence, by tuning the distortion damping resistance, the contribution of each DG  
 372 unit in the unbalance sharing can be affected.

373 In the previous, the assumption of purely resistive lines was made. In Fig. 6, the results are shown  
 374 for the same case as above, but with additional inductance in the lines such that  $R/X=1$  (which is  
 375 unrealistically low in a low-voltage microgrid). Still, a stable microgrid operation is obtained. The  
 376 transients take slightly less time as the total line impedance becomes  $\sqrt{2}$  times the previous line  
 377 resistance. However, the settling time of voltage in Fig. 6(b) is clearly longer. As assumed above, it  
 378 is shown here that the effect of not purely resistive lines on the VBD control operation and the unbalance  
 379 is limited.

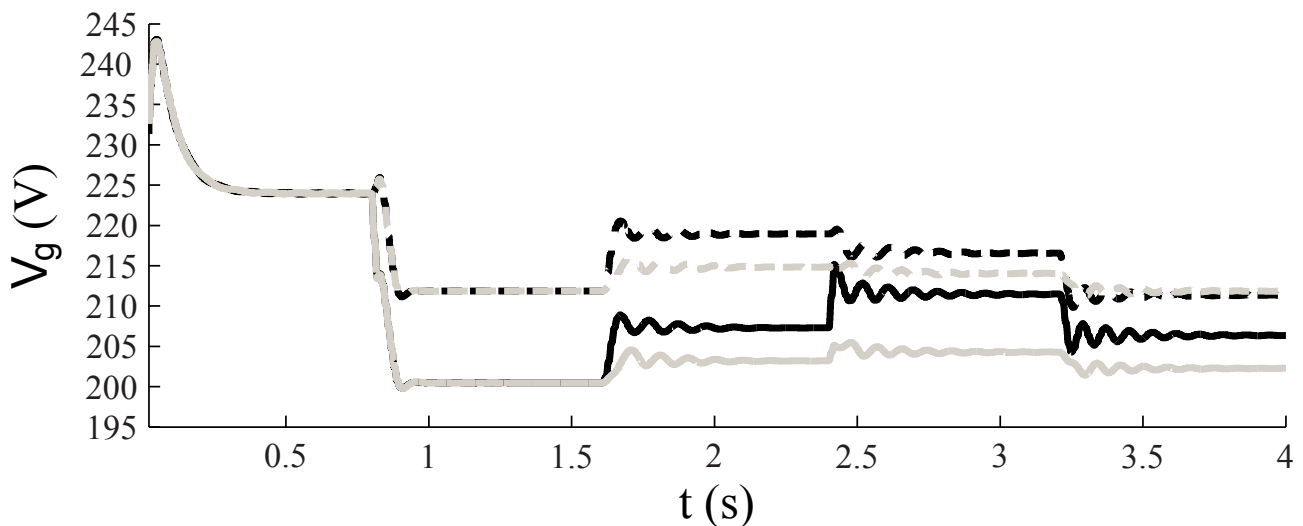
#### 380 5.5. Discussion

381 When considering only one DG unit with distortion damping resistance, the CW method is generally  
 382 most beneficial but attention should be paid as it provides less damping in the system. For achieving

**Figure 5.** Dynamic simulation (— = DG 1/ phase a, - - - = DG 1/phases b and c, — (gray)= DG 2/phase a, - - - (gray)= DG 2 /phases b and c )



(a) Output power  $P$



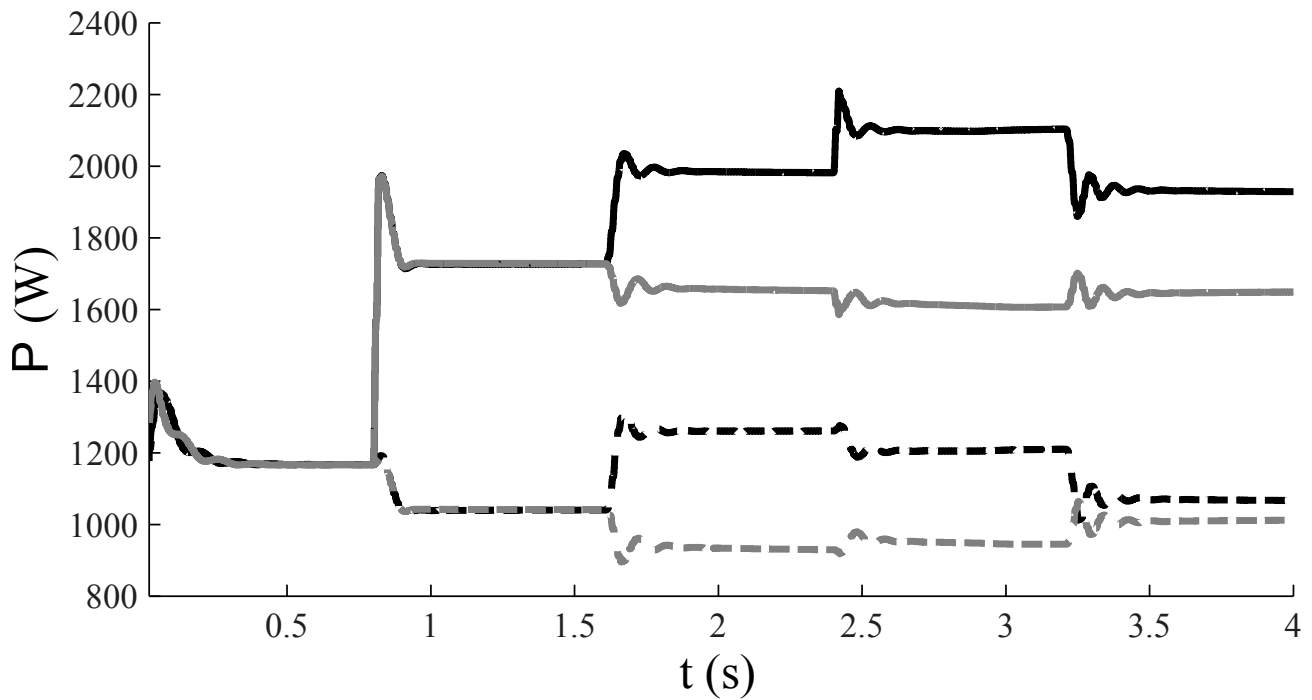
(b) Terminal voltage  $V_g$

383 actively controlled unbalance sharing between multiple DG units, the RU method is generally most  
 384 beneficial, mainly because of its damping effect. The unit with the smallest  $R_d$  contributes most in the  
 385 unbalance sharing.

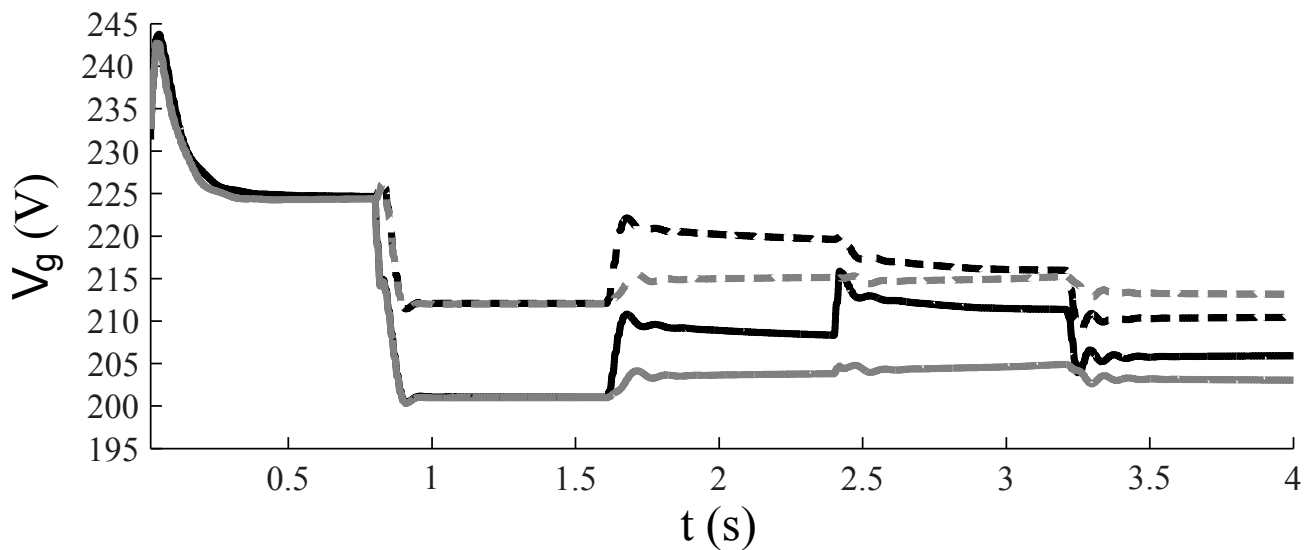
## 386 6. Conclusions

387 In this paper, the VBD control is modified for application in three-phase networks. This controller  
 388 achieves a stable three-phase islanded microgrid operation and has the same benefits as its single-phase  
 389 variant. An additional control loop is added, with as characterizing parameter the distortion damping  
 390 resistance, in order to actively control the effect of the DG units on the unbalance in the microgrid. A  
 391 comparison is made between positive and negative values of this resistance. It is shown that the value  
 392 of the distortion damping resistance can affect the voltage unbalance factor at the load and the line

**Figure 6.** Dynamic simulation with inductance in the lines (— = DG 1/ phase a, - - - = DG 1/phases b and c, — (gray)= DG 2/phase a, - - - (gray)= DG 2 /phases b and c )



(a) Output power  $P$



(b) Terminal voltage  $V_g$

393 losses in the microgrid. A trade-off between these two parameters should be made. By properly setting  
 394 the distortion damping resistance, e.g., according to the ratings of the DG units, the unbalance sharing  
 395 between the DG units can be actively controlled.

### 396 Acknowledgements

397 The research was carried out in the frame of the Inter-university Attraction Poles program IAP-VII-02,  
398 funded by the Belgian Government. The research of J. D. M. De Kooning and T. Vandoorn is funded by  
399 the Special Research Fund (BOF) of Ghent University (Belgium).

#### 400 **Conflicts of Interest**

401 The authors declare no conflict of interest.

#### 402 **References**

- 403 1. Energy, S. Microgrids key to the Smart Grid's evolution. *www.powerengineeringint.com* **2010**.
- 404 2. Fang, X.; Misra, S.; Yang, G.X.D. Smart Grid - The New and Improved Power Grid: A Survey.  
405 *IEEE Commun. Surveys Tuts.* **2012**, *14*, 944–980.
- 406 3. Bhaskara, S.; Chowdhury, B. Microgrids - A review of modeling, control, protection, simulation  
407 and future potential. Power and Energy Society General Meeting, 2012 IEEE, 2012, pp. 1–7.
- 408 4. Lasseter, R.H.; Paigi, P. Microgrid: A Conceptual Solution. Proc. IEEE Power Electron. Spec.  
409 Conf. (PESC 2004); , 2004.
- 410 5. Engler, A.; Osika, O.; Barnes, M.; Hatziargyriou, N. *DB2 Evaluation of the local controller*  
411 *strategies*; www.microgrids.eu/micro2000, 2005.
- 412 6. Vandoorn, T.L.; Meersman, B.; Degroote, L.; Renders, B.; Vandeveldel, L. A Control Strategy for  
413 Islanded Microgrids with dc-link Voltage Control. *IEEE Trans. Power Del.* **2011**, *26*, 703–713.
- 414 7. Meersman, B.; Renders, B.; Degroote, L.; Vandoorn, T.; Vandeveldel, L. Three-phase inverter-  
415 connected DG-units and voltage unbalance. *Electric Power Systems Research* **2011**, *81*, 899–906.
- 416 8. Guerrero, J.M.; Loh, P.C.; I. Lee, T.; Chandorkar, M. Advanced Control Architectures for Intelligent  
417 Microgrids- Part II: Power Quality, Energy Storage, and AC/DC Microgrids. *IEEE Trans. Ind.*  
418 *Electron.* **2013**, *60*, 1263–1270.
- 419 9. Renders, B.; De Gussemé, K.; Ryckaert, W.R.; Vandeveldel, L. Converter-Connected Distributed  
420 Generation Units with Integrated Harmonic Voltage Damping and Harmonic Current Compensation  
421 Function. *Electric Power Systems Research* **2009**, *79*, 65–70.
- 422 10. Vasquez, J.; Guerrero, J.; Savaghebi, M.; Eloy-Garcia, J.; Teodorescu, R. Modeling, Analysis,  
423 and Design of Stationary Reference Frame Droop Controlled Parallel Three-Phase Voltage Source  
424 Inverters. *IEEE Trans. Ind. Electron.* **2013**, *60*, 1271–1280.
- 425 11. Katiraei, F.; Iravani, R.; Hatziargyriou, N.; Dimeas, A. Microgrids Management: controls and  
426 operation aspects of microgrids. *Power and Energy Magazine* **2008**, *6*, 54–65.
- 427 12. Guerrero, J.M.; Vásquez, J.C.; Matas, J.; de Vicuña, L.G.; Castilla, M. Hierarchical Control of  
428 droop-controlled AC and DC microgrids - A general approach towards standardization. *IEEE*  
429 *Trans. Ind. Electron.* **2011**, *58*, 158–172.
- 430 13. Mohamed, Y.A.R.I.; El-Saadany, E.F. A Control Scheme for PWM Voltage-Source Distributed-  
431 Generation Inverters for Fast Load-Voltage Regulation and Effective Mitigation of Unbalanced  
432 Voltage Disturbances. *IEEE Trans. Ind. Electron.* **2008**, *55*, 2072–2084.
- 433 14. Cheng, P.T.; Chen, C.A.; Lee, T.L.; Kuo, S.Y. A Cooperative Imbalance Compensation Method for  
434 Distributed-Generation Interface Converters. *IEEE Trans. Ind. Appl.* **2009**, *45*, 805–815.

- 435 15. Savaghebi, M.; Jalilian, A.; Vasquez, J.C.; Guerrero, J.M. Autonomous voltage unbalance  
436 compensation in an islanded droop-controlled microgrid. *IEEE Trans. Ind. Electron.* **2013**,  
437 *60*, 1390–1402.
- 438 16. Hamzeh, M.; Karimi, H.; Mokhtari, H. A neg control strategy for a multi-bus MV microgrid under  
439 unbalanced conditions. *IEEE Trans. Power Syst.* **2012**, *27*, 2225–2232.
- 440 17. Savaghebi, M.; Jalilian, A.; Vasquez, J.C.; Guerrero, J.M. Secondary Control for Voltage Quality  
441 Enhancement in Microgrids. *IEEE Trans. on Smart Grid* **2013**, *3*, 1893–1902.
- 442 18. Renders, B.; De Gussemé, K.; Ryckaert, W.R.; Vandeveld, L. Input Impedance of Grid-Connected  
443 Converters with Programmable Harmonic Resistance. *IET Electr. Power Appl.* **2007**, *1*, 355–361.
- 444 19. De Gussemé, K.; Ryckaert, W.R.; Van de Sype, D.M.; Ghijsselen, J.A.; Melkebeek, J.A.;  
445 Vandeveld, L. A boost PFC converter with programmable harmonic resistance. *IEEE Trans.*  
446 *Ind. Appl.* **2007**, *43*, 742–750.
- 447 20. Pogaku, N.; Green, T. Application of Inverter-Based Distributed Generators for Harmonic Damping  
448 Throughout a Distribution Network. Proc. IEEE Power Electr. Spec. Conf. (PESC'05).
- 449 21. Takeshita, T.; Matsui, N. Current waveform control of PWM Converter system for harmonic  
450 suppression on distribution system. *IEEE Trans. Ind. Electron.* **2003**, *50*, 1134–1139.
- 451 22. Yao, W.; Chen, M.; Guerrero, J.M.; Qian, Z.M. Design and analysis of the droop control method  
452 for parallel inverters considering the impact of the complex impedance on the power sharing. *IEEE*  
453 *Trans. Ind. Electron.* **2011**, *58*, 576–588.
- 454 23. Guerrero, J.M.; García de Vicuña, L.; Matas, J.; Castilla, M.; Miret, J. Output Impedance design  
455 of parallel-connected UPS inverters with wireless load-sharing control. *IEEE Trans. Ind. Electron.*  
456 **2005**, *52*, 1126–1135.
- 457 24. Engler, A.; Soutanis, N. Droop Control In LV-Grids. Proc. Internat. Conf. on Future Power  
458 Systems; , 2005.
- 459 25. Vandoorn, T.L.; Renders, B.; Degroote, L.; Meersman, B.; Vandeveld, L. Active Load Control in  
460 Islanded Microgrids based on the Grid Voltage. *IEEE Trans. on Smart Grid* **2011**, *2*, 139–151.
- 461 26. Vandoorn, T.L.; Meersman, B.; De Kooning, J.D.M.; Vandeveld, L. Transition from Islanded to  
462 Grid-Connected Mode of Microgrids with Voltage-Based Droop Control. *IEEE Trans. Power Syst.*  
463 **2013**, *28*, 2545–2553.